Proceedings of the 3rd International Conference on Mechanical Engineering and Mechatronics
Prague, Czech Republic, August 14-15, 2014
Paper No. 67

Cryogenic Throttle Valve Driven by BLDC Motor for Thrust Control of a Liquid Rocket Engine

Taekyu Jung, SangYeop Han
Korea Aerospace Research Institute
169-84, Gwahangno, Daejeon, Republic of Korea
tkjung@kari.re.kr; syhan@kari.re.kr

Abstract **-** This paper presents the activities performed for the development of a cryogenic throttle valve which was designed for the thrust control of an LRE. The throttle valve can adjust the flow rate of liquid oxygen under a cryogenic temperature of 90K and a high pressure of 113.2bar with the help of an electro-mechanical actuator driven by a BLDC motor. All development tests have been performed except engine firing test. The mathematical model and control algorithm of the throttle valve were described as a preliminary study on the design of thrust control algorithm for an LRE. The mathematical models of the throttle valve including a controller and a thrust control simulator have been developed. The dynamic characteristics predicted by the mathematical models showed good agreement with experimental results, thus proving the validity of the mathematical models. It was also found that an optimum control algorithm of the throttle valve for a thrust control simulator is an On-Off control.

***Keywords*:** Thrust Control, Throttle Valve, LRE.

Nomenclature

CMD	=	command voltage transferred from PID controller to motor driver for the control of motor speed (V)
EMA	=	electro-mechanical actuator
e_a	=	applied voltage to motor (V)
e_b	=	back emf (V)
G	=	specific gravity
i_a	=	motor armature current (A)
J	=	moment of inertia (kg-m^2)
K_b	=	coefficient of back emf (V-s/rad)
K_I	=	integral gain
K_p	=	proportional gain
K_t	=	torque constant (Nm/A)
K_v	=	flow coefficient
L_a	=	terminal inductance (phase to phase, H)
ΔP	=	pressure drop (bar)
Q	=	flow rate (m^3/h)
R_a	=	terminal resistance of motor (phase to phase, ohm)
TCV	=	thrust control valve (throttle valve in this paper)
T_e	=	motor torque (Nm)
T_L	=	load torque (Nm)
θ	=	angular displacement of the motor (radian)
θ_s	=	angular displacement of the valve shaft (radian)
ω	=	angular velocity of the motor (radian)

1. Introduction

A throttle valve is widely used to control the thrust level of a liquid rocket engine (LRE) by adjusting the flow rate of a propellant entering a gas-generator or pre-burner. In the rocket industry, most throttle valves use DC motors as their actuators (Borbouse et al., 2002 and MaCormick et al., 2006) because DC motors are more simple, more controllable, lighter, more reliable and safer than conventional pneumatic, hydraulic actuators. In this paper, a cryogenic throttle valve driven by a BLDC motor is introduced, which is being developed for the thrust control of a liquid propellant rocket engine. Comprehensive mathematical models of the valve including a controller and a test facility are developed. An optimized control algorithm for the valve is proposed. Also, experimental results are compared with simulation results by mathematical models.

The LRE is a so-called "open cycle engine" with a fuel-rich gas-generator as shown in Fig. 1. In this engine, a thrust control valve (TCV) is installed in the oxidizer line of the gas-generator to modulate the hydraulic resistance because the fuel flow rate of the gas-generator is larger than that of the oxidizer.

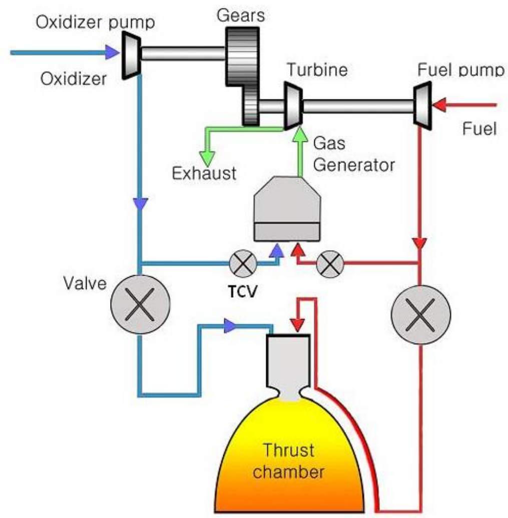

Fig. 1. Simplified scheme of the fuel-rich open cycle engine.

Fig. 2. Throttle valve.

2. Throttle Valve and Controller

2. 1. Throttle Valve

Fig. 2 shows the throttle valve. All development tests have been performed successfully except for a firing test on an LRE. The throttle valve comprises a flow control part and an EMA (Electro-Mechanical-Actuator). The flow control part is composed of a shaft, a sleeve and a plunger as shown in Fig. 3(a). The sleeve moves horizontally in accordance with the rotation of the shaft connected to the EMA, and then the flow area between the sleeve and plunger is changed to adjust the flow rate of liquid oxygen. This kind of valve type is called an in-line co-axial valve (Horstmann et al., 1999). This valve has a thin sleeve, resulting in small flow-induced force acting on the end tip of the sleeve. Therefore, the required power of the EMA is very small compared to other types of valves such as ball and globe valves. This advantage makes the valve smaller and lighter. Therefore, in-line co-axial valves are widely used in an LRE as shown by MaCormick et al. (2006), Horstmann et al. (1999) and Jung et al. (2010). The EMA comprises a BLDC motor, speed reduction gears, a torque limiter, a potentiometer and other components, as shown in Fig. 3(b). The torque limiter can protect the motor and gears against overload if the sleeve and shaft become stuck due to some mechanical malfunction. The torque limiter makes the motor run idle when the torque of the shaft exceeds a design limit. The potentiometer can measure the rotational angle of the shaft. Therefore the signal from the potentiometer can be used to control the position of the shaft or sleeve. The main specifications of the throttle valve are given in Table. 1.

2. 2. Controller of Throttle Valve

The controller was fabricated with industrial electronic elements to obtain the maximum flexibility. In fact, the controller is not supposed to fly. So the requirements for the electronic controller are only compatible with a laboratory environment. Fig. 4 shows the controller. The controller can control three throttle valves at the same time. It can control the speed of the motors and valve position. It comprises an embedded real-time controller such as cRIO 9014 and three motor drivers (amplifiers). Also, the controller can acquire data on not only the motor status, but also the pressure and flow rates of the hydraulic lines in a test facility to control the throttle valve according to a control algorithm.

A computer communicates with the controller via TCP/IP. It gives control orders to the controller and takes data from the controller at a 100Hz sampling rate. The control S/W is programmed using Labview.

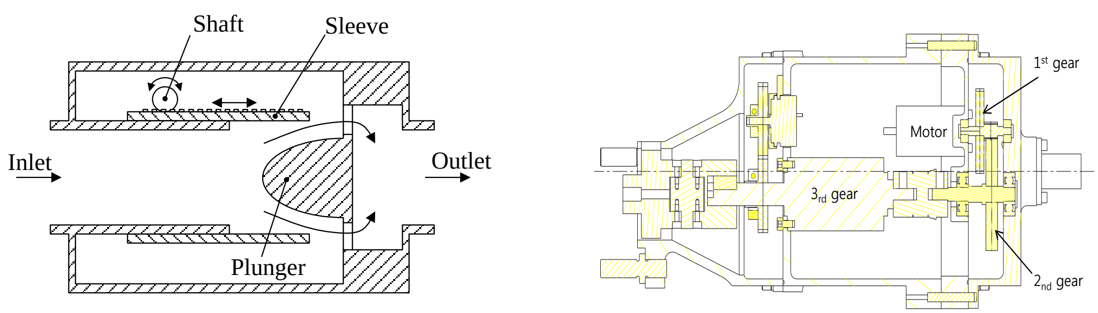

(a) Flow control part (b) EMA

Fig. 3. Cross-section of throttle valve.

Table. 1. Specification of throttle valve.

Specification	Unit	Value
Flow diameter	mm	14.4
Medium	-	LOx
Flow rate (Nom.)	kg/s	3.1
Pressure (Max.)	bar	113.2
Temperature	K	90-300
Voltage	V	24
External leakage	scc/sec GHe	$<10^{-3}$
Weight	kg	3.1
Gear ratio	-	1,584

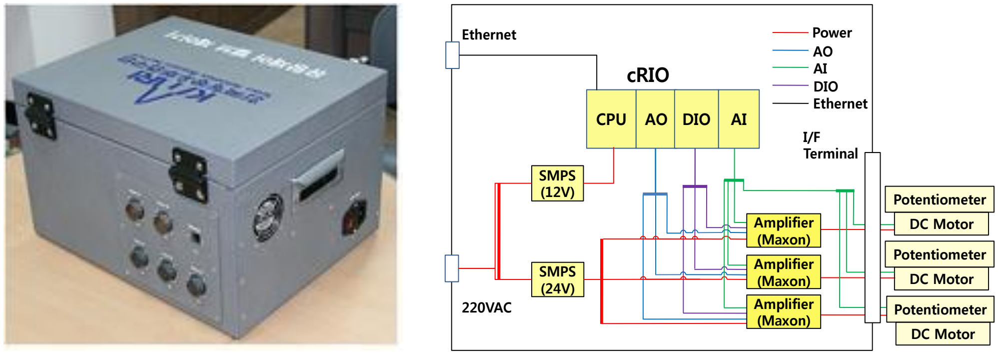

Fig. 4. Controller of throttle valve.

3. Development Test

3. 1. Flow Characteristic Test

Fig. 5 shows the experimental result of the inherent flow characteristic of the throttle valve along the valve position (shaft angle). The flow coefficient, K_v is defined as follows:

$$K_v = Q\sqrt{\frac{G}{\Delta P}} \quad (1)$$

The shape of K_v can be designed in accordance with the profile of the plunger shown in Fig. 3(a). In general, the profile of the plunger is designed so that the thrust gain, $\delta T/\delta\theta$ (T: engine thrust, θ: shaft angle) can be held constant. The constant thrust-gain enables the effective thrust control of an LRE.

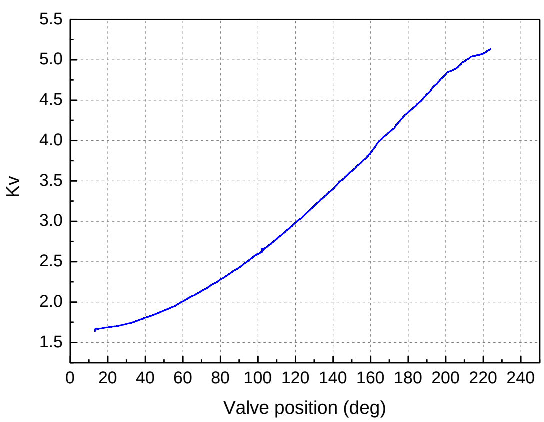

Fig. 5. Inherent flow characteristic of throttle valve.


Fig. 6. Cryogenic leakage and function test.

3. 2. Pressure Proof and Leakage Test

A pressure proof test was performed under 170 bar using water. There was no permanent deformation and leakage during the test. Also, leakage tests were performed successfully under 125 bar using GHe at a room temperature and a cryogenic temperature of 90K. The cryogenic test was performed in an LN_2 submersion tank as shown in Fig. 6. During the cryogenic leakage test, a functional test was also performed without any problem.

Fig. 7. EMI test.

Fig. 8. Vacuum environment test.

3. 3. EMI and Vacuum Test

Many kinds of electronic equipment are installed in a launch vehicle. Therefore, the EMI test of the throttle valve was performed as shown in Fig. 7. The strength of electromagnetic wave was measured according to MIL-STD-461(RE102). The measured amplitude of the electromagnetic wave was 20dB lower than the allowable level.

A satellite launch vehicle is exposed to vacuum environment during flight. Therefore a vacuum environment test of the throttle valve was performed at 10^{-3} torr as shown in Fig. 8. The vacuum test was performed successfully without any problem. In fact, the BLDC motor does not have brushes and works under low voltage (24V), so that problems such as corona discharge and spark on brushes are not encountered.

3. 4. Vibration Test

Vibration tests of the throttle valve were performed as shown in Fig. 9 along the x, y, and z axes. After and during all vibration tests such as acceleration, random, sinusoidal and pyro-shock test, the throttle valve worked normally and did not show any damage.

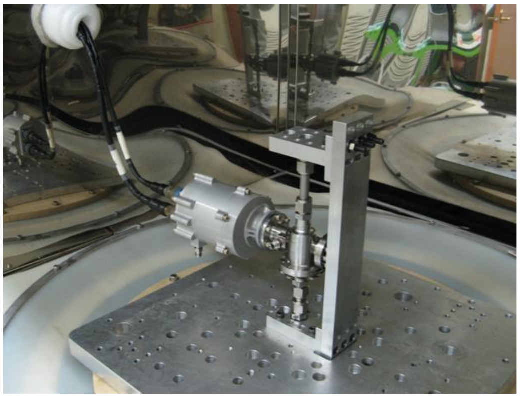

Fig. 9. Vibration test.

3. 5. Durability Test

Durability tests were performed as follows.

- 100 cycles, 125 bar at room temperature.
- 50 cycles, 125 bar in an LN_2 submersion tank as shown in Fig. 6.

After each durability test, leakage tests were performed successfully. The leakage was within the allowable limit. Also, the change of hysteresis of K_v before and after the durability test was within 0.5%.

4. Mathematical Model of the Throttle Valve

The mathematical model for the throttle valve including the EMA and motor driver was established for simulation and comparison with experiment. The model of the throttle valve is derived on the basis of the governing equation of the general DC motor as follows:

$$L_a \frac{di_a}{dt} + R_a i_a + e_b = L_a \frac{di_a}{dt} + R_a i_a + K_b \frac{d\theta}{dt} = e_a \tag{2}$$

$$J \frac{d^2\theta}{dt^2} + b \frac{d\theta}{dt} + T_L = T_e = K_t i_a \tag{3}$$

Fig. 10 shows the mathematical model of the throttle valve including the motor driver. The motor driver controls motor-speed using a PI controller. The PI controller denoted by G(s) in Fig. 10 is expressed as Eqn. (4). In general, the proportional controller is responsible for dynamic response, and the integral controller is for steady-state accuracy.

$$G(s) = K_p + \frac{K_I}{s} \tag{4}$$

The mathematical model of Fig. 10 was validated using experimental data. Figure 11 shows the simulated and experimental results for the motor response under the command voltage of 5V (CMD 5V result in a motor speed of 7500 rpm, CMD 0V result in motor stop). The simulation result using MATLAB/Simulink shows good agreement with the experimental result, thus proving the validity of the mathematical model of the throttle valve and motor driver.

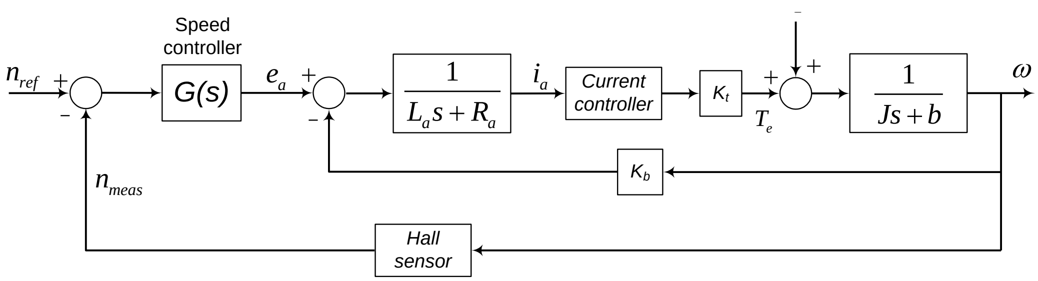

Fig. 10. Block diagram of throttle valve and motor driver model.

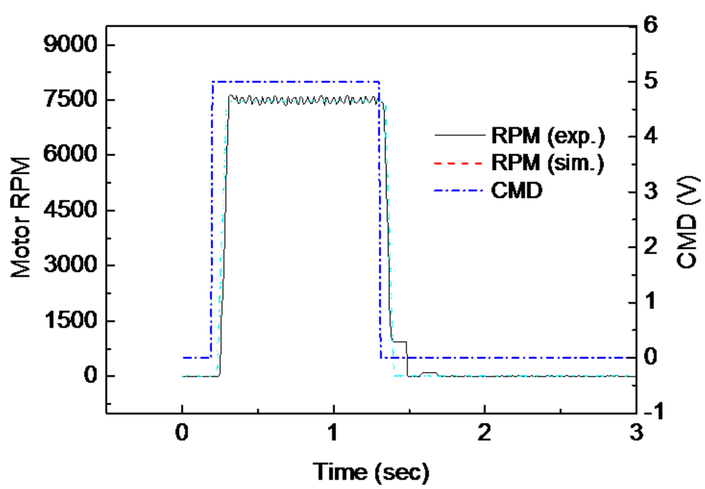

Fig. 11. Simulation and experimental results for motor function test under CMD 5V

5. Control Algorithm of Throttle Valve

5.1. Thrust Control Simulation

As a preliminary study on the thrust control algorithm for an LRE, the control algorithm of the throttle valve was validated in a thrust control simulator as shown in Fig. 12. The run tank is filled with water and pressurized with 50 bar of nitrogen gas by a pneumatic pressure regulator. A solenoid valve (S/V) before the throttle valve (TCV) is installed to generate the step pressure at the inlet port of the throttle valve.

5.2. Mathematical Model of the Simulator

The mathematical model of the simulator was developed. The model comprises the throttle valve and pipe system after the throttle valve. The model can be expressed with a block diagram as shown in Fig. 13. The PID controller and motor driver are components of the controller (Fig. 4). The perturbation of inlet pressure, δP_1, which is generated by opening S/V, is used as a disturbance input. The model was simulated using MATLAB/Simulink. δP_1=1 bar and $\delta P_{2\text{-ref}}$ =0 bar were used as the input data.

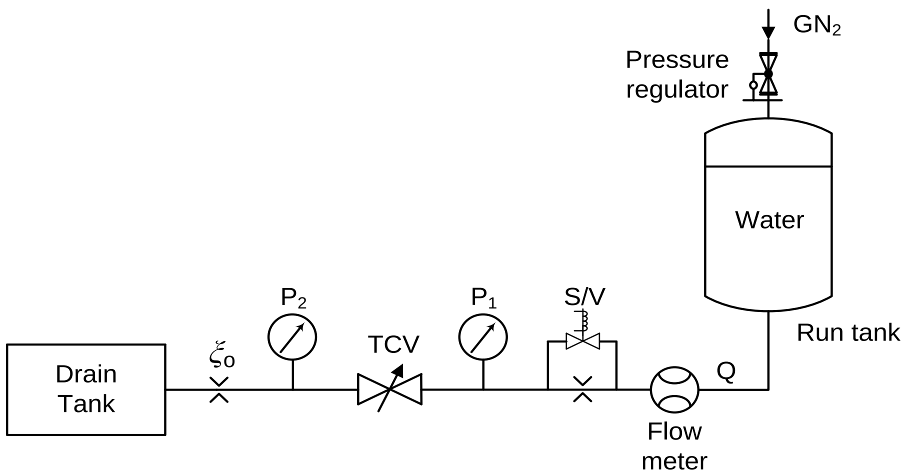

Fig. 12. Schematic of thrust control simulator.

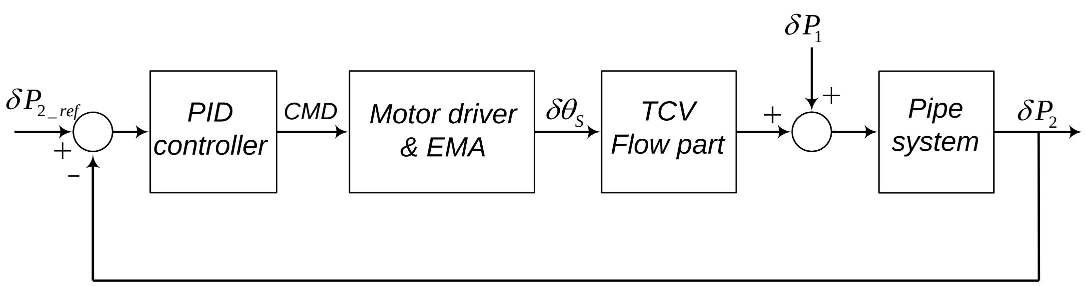

Fig. 13. Block diagram of thrust control simulator.

5.3. Control Algorithm

The optimum control algorithm for this simulator was studied. PI controller, which I-gain is fixed with '1', shows overshoot and steady-state error as shown in Fig. 14(a). However, the P controller shows good control performance as P-gains increase as shown in Fig. 14(b).

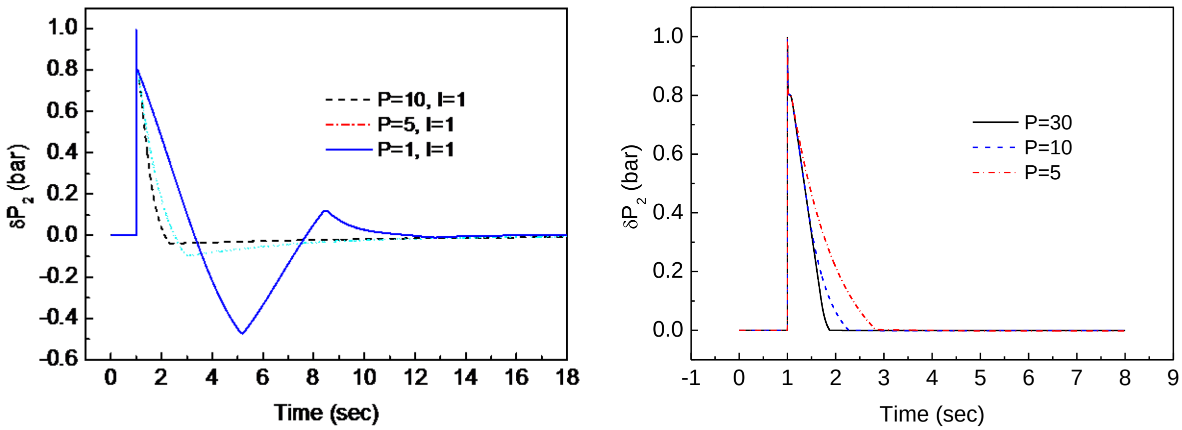

(a) Outlet pressure, δP_2 (PI controller) (b) Outlet pressure, δP_2 (P controller)

Fig. 14. Simulation result for δP_2 under disturbance of δP_2= 1 bar.

The outlet pressure, P_2, is measured by a pressure transducer. All signals from transducers have some noise and signal fluctuations. In this research, the threshold of '$|\delta P_{2\text{-ref}} - \delta P_2| < T_{th}$' was used as the stop condition of the motor to prevent useless operation of the throttle valve due to sensor noise. Fig. 15 shows simulation results along the increase of P-gains with T_{th}=0.1 bar. It can be seen in Fig. 15(a) that the larger the P-gain is, the better performance the system shows. When P gains are over 30, the command voltage and motor RPM are almost the same regardless of P-gain as shown in Fig. 15(b,c). This means that if only P-gain is large enough, then the P controller works like an On-Off controller. Therefore, it was found that the optimum control algorithm for the simulator is an On-Off control.

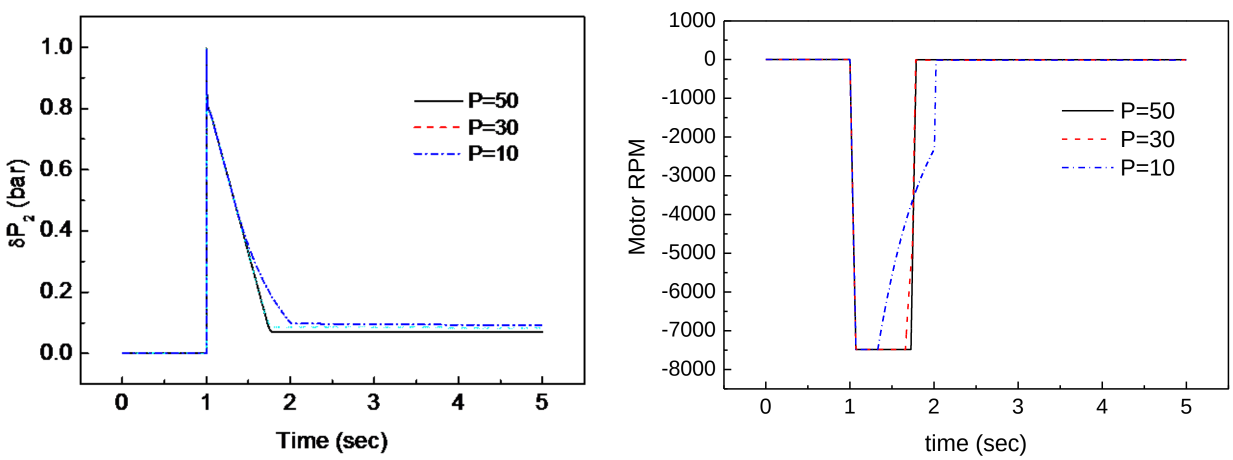

(a) Outlet pressure, δP_2 (b) Motor RPM

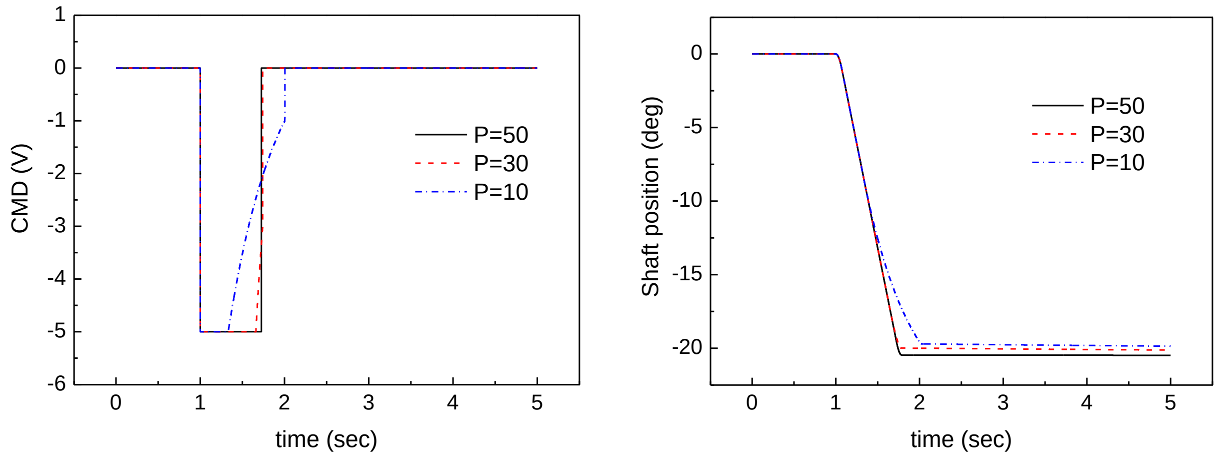

(c) Command voltage (d) Shaft angle of throttle valve

Fig. 15. Simulation result by P control with T_{th}=0.1 bar.

5.4. Simulation and Experiment

To validate the mathematical model of the thrust control simulator and the On-Off control algorithm for the throttle valve, the block diagram shown in Fig. 13 was solved using MATLAB/Simulink and compared with the experimental result as shown in Fig. 16. The experiment was performed as follows. The solenoid valve (S/V) in Fig. 12 is opened at 10.13 second; then the inlet pressure (P_1) is increased abruptly. The controller was programmed for the throttle valve to maintain the outlet pressure at 15 bar, which is the same pressure before opening the solenoid valve. The experimental data of P_1 was used as the input data for the simulation. The threshold, T_{th}=0.2 bar, was used for both of simulation and experiment. P-gain of 50 was used for the PID controller to work as if it is an On-Off controller. In Fig. 16(a), the simulation result on P_2 shows good agreement with the experimental result, thus proving the validity of the mathematical model. Fig. 16(b) shows the measured data of control variables (CMD, error signal) and motor RPM. Error signal means 'P_{2_ref}-P_2'. It can be seen that CMD 5V is released exactly when the error signal exceeds T_{th} and CMD 0V is released exactly when the error signal is within T_{th}. These result shows that the On-Off control algorithm of the throttle valve can control the outlet pressure effectively. In an LRE, the control target for the thrust control is the pressure of the combustion chamber. The outlet pressure of the throttle valve is linearly proportional to the pressure of the combustion chamber. Therefore the On-Off control algorithm of the throttle valve can control the thrust of an LRE effectively.

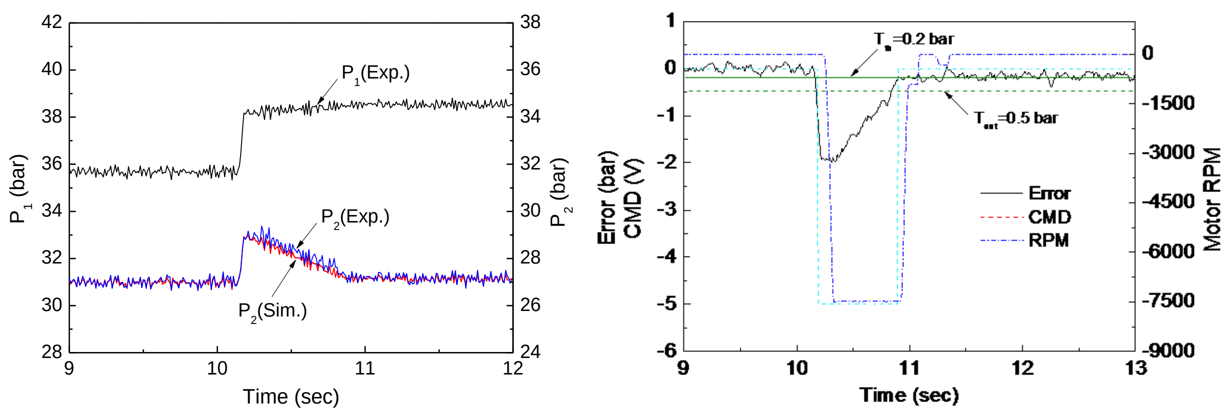

(a) Simulation and experiment result for P_2 (b) Experiment result for CMD, RPM, error signal

Fig. 16. Outlet pressure control on thrust control simulator.

6. Conclusion

Activities for the development of a cryogenic throttle valve, which was developed for the thrust control of a liquid propellant rocket engine, were summarized in this paper. Comprehensive mathematical models of the throttle valve including a controller and a thrust control simulator were developed. It was found that an optimized control algorithm for the throttle valve is an On-Off control. Simulations and experiments were conducted to verify the mathematical models. The simulation results agreed well with the experimental results. The mathematical models introduced in this paper can be used to predict performance and to provide insight for improving the design of the throttle valve and thrust control algorithm for an LRE. They will be also useful in the design and analysis of LREs that use this kind of throttle valve.

References

MaCormick S. and Garrison M. (2006). EM Actuated Cryogenic Valve for Engine Control. "AIAA 2006-4881, 42nd AIAA/ASME/SAE/ASEE Joint Propulsion Conference & Exhibit," California, USA, July 9-12.

Borbouse C., Jauquet P.F., Bomal J.C. and Promper C. (2002). Electronically Controller Ball Valve: the Lox Valve of Vinch. "4th International Conference on Launcher Technology," Liege, Belgium, Dec. 3-6.

Horstmann M. and Routh M. (1999). Status of Dasa Development of Motor Driven Valves. "35th AIAA/ASME/SAE/ASEE Joint Propulsion Conference & Exhibit," AIAA-99-2331, California, USA, June 20-24.

Jung T. and Lee S. (2010). Development of BLDC Motor Driven Cryogenic Thrust Control Valve for Liquid Propellant Rocket Engine. "The Korean Society for Aerospace and Space Sciences," Vol. 38, No. 10, pp. 1026-1030.